Photochemical & Photobiological Sciences

Accepted Manuscript

This is an *Accepted Manuscript*, which has been through the Royal Society of Chemistry peer review process and has been accepted for publication.

Accepted Manuscripts are published online shortly after acceptance, before technical editing, formatting and proof reading. Using this free service, authors can make their results available to the community, in citable form, before we publish the edited article. We will replace this *Accepted Manuscript* with the edited and formatted *Advance Article* as soon as it is available.

You can find more information about *Accepted Manuscripts* in the Information for Authors.

Please note that technical editing may introduce minor changes to the text and/or graphics, which may alter content. The journal's standard Terms & Conditions and the Ethical guidelines still apply. In no event shall the Royal Society of Chemistry be held responsible for any errors or omissions in this *Accepted Manuscript* or any consequences arising from the use of any information it contains.

ROYAL SOCIETY OF CHEMISTRY

www.rsc.org/pps

Subtle Structural Changes in Octupolar Merocyanine Dyes Influence the Photosensitized Production of Singlet Oxygen†

Mikkel Bregnhøj,[a] Frederico M. Pimenta,[a] Yevgen M. Poronik,[b] Daniel T. Gryko,*[b] and Peter R. Ogilby*[a]

[a] Center for Oxygen Microscopy and Imaging, Department of Chemistry, Aarhus University, Aarhus, 8000 Denmark. E-mail: progilby@chem.au.dk

[b] Institute of Organic Chemistry of the Polish Academy of Sciences, 01-224 Warsaw, Poland. E-mail: dtgryko@icho.edu.pl

†Electronic Supplementary Information (SI) available: NMR spectra and X-Ray crystallographic data of compounds synthesized.

Abstract

The photophysical properties of two indoline-based octupolar merocyanine dyes and of the corresponding quinoline-based dyes were examined. This seemingly subtle structural change in the chromophore of these molecules has an appreciable effect on the yields with which these respective compounds sensitize the production of singlet molecular oxygen, $O_2(a^1\Delta_g)$. The indoline-based dyes are reasonably efficient $O_2(a^1\Delta_g)$ sensitizers ($\phi_\Delta \sim 0.35$), whereas the quinoline-based dyes are poor $O_2(a^1\Delta_g)$ sensitizers ($\phi_\Delta \sim 0.005$). A series of experiments, including Laser-Induced Optoacoustic Calorimetric (LIOAC) measurements, reveal that this difference principally reflects the fact that the excited singlet state of the quinoline-based dyes rapidly and efficiently decays via nonradiative channels to regenerate the ground state molecule. It is likely that a charge-transfer state mediates this efficient coupling between the excited and ground states. Such subtle, structure-dependent effects are important in elucidating and ultimately understanding phenomena that influence the efficiency of photosensitized $O_2(a^1\Delta_g)$ production. In turn, the knowledge gained facilitates the rational design and preparation of $O_2(a^1\Delta_g)$ sensitizers with explicitly-controlled properties.

Introduction

The photosensitized production of singlet oxygen, $O_2(a^1\Delta_g)$, continues to be a topic of interest from many perspectives. It is an important natural process that routinely occurs in our world of light, oxygen and chromophores.[1, 2] From the perspective of a practical application, its use as a clinical tool to perturb tissue and cells has certainly garnered the spotlight over the past ~ 30 years. For example, in photodynamic cancer treatments, the photosensitizer is administered as the drug, and a great effort has been expended to develop suitable molecules for this purpose.[3] From a fundamental mechanistic perspective, much remains to be learned about molecular phenomena that determine the efficiency of energy transfer from the excited state sensitizer to ground state oxygen, $O_2(X^3\Sigma_g^-)$, to produce $O_2(a^1\Delta_g)$.[4] Of particular interest in this regard, certainly in complicated biological systems, is the extent to which photoinitiated electron transfer processes compete with the energy transfer process.[5]

Over the years, thousands of molecules have been examined from the viewpoint of their ability to photosensitize the production of $O_2(a^1\Delta_g)$.[6, 7] Although much is indeed known about what molecular features are conducive to the efficient photosensitized production of singlet oxygen,[4] the community continues to encounter new data and challenges that are not easily understood. In the least, the latter remind us that much must still be accomplished before a given $O_2(a^1\Delta_g)$ photosensitizer can be systematically designed and prepared for a given purpose.

In recent work on the merocyanine derivatives shown in Fig. 1, we discovered that the apparently subtle structural changes in the nitrogen heterocyclic moiety result in an appreciable change in the yield of photosensitized $O_2(a^1\Delta_g)$. Because an immediate explanation for this observation was not available, we set out to explore this issue further. The results of this study are reported herein.

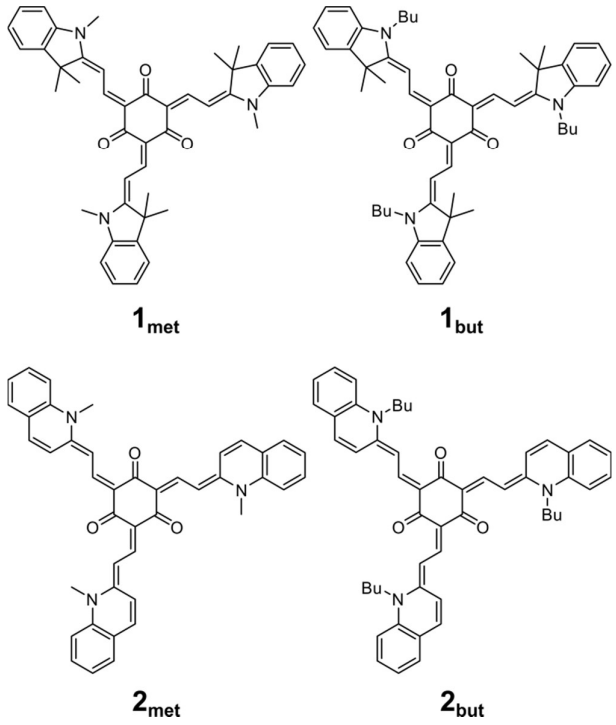

Fig. 1. Structures of the four merocyanine dyes examined in this study

Experimental

Chemicals. HPLC-grade toluene, HPLC-grade N,N-dimethylformamide, azulene (99%), *meso*-tetraphenylporphyrin (99%), tetrabutylammonium tetrafluoroborate (99%), and ferrocene (99%) were all obtained from Sigma-Aldrich and used as received. Phenalenone, PN (97%, Sigma-Aldrich) was recrystallized twice from ethanol before use.

2,4,6-tris((*E*)-2-(1,3,3-trimethylindolin-2-ylidene)ethylidene)-cyclohexane-1,3,5-trione, $\mathbf{1}_{\mathbf{met}}$, and the related butylated quinoline-derived compound, $\mathbf{2}_{\mathbf{but}}$, were synthesized according to a previously published procedure.[8] The corresponding compounds $\mathbf{1}_{\mathbf{but}}$ and $\mathbf{2}_{\mathbf{met}}$ were synthesized using the approach shown in Scheme 1 and described below. For these procedures, all chemicals were used as received unless otherwise noted. Reagent grade solvents (CH_2Cl_2, hexane) were

distilled prior to use. Chromatography was performed on silica gel (230-400 mesh) or neutral aluminum oxide (70-230 mesh).

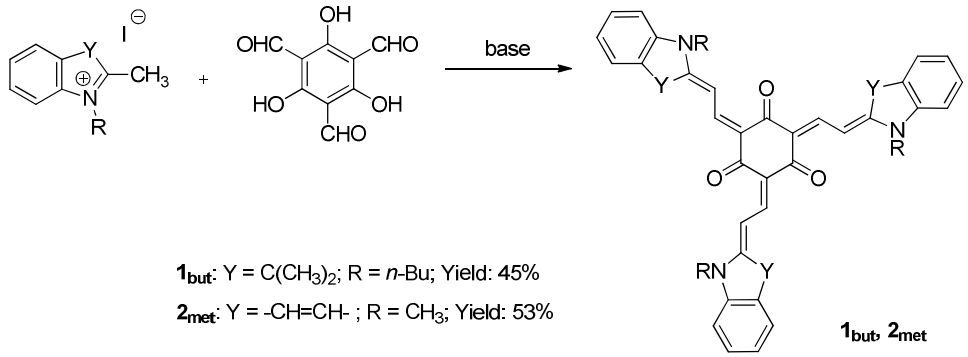

Scheme 1. Methodology used to synthesize $\mathbf{1_{but}}$ and $\mathbf{2_{met}}$.

2,4,6-tris((E)-2-(1-butyl-3,3-dimethylindolin-2-ylidene)ethylidene)cyclohexane-1,3,5-trione, $\mathbf{1_{but}}$: The mixture of 1-butyl-2,3,3-trimethyl-3H-indol-1-ium iodide[9] (0.57 g, 1.65 mmol) and 2,4,6-trioxocyclohexane-1,3,5-tricarbaldehyde[10] (0.11 g, 0.5 mmol) in 3 ml of pyridine was refluxed for 5 min. After cooling, the reaction was diluted with 40-50 ml of diethyl ether. The solvents were decanted and the oily material was washed several times with diethyl ether. The crude product was eluted through silica gel (CH_2Cl_2-CH_3OH, 95:5) and the solvent removed by evaporation. The residue was recrystallized from cyclohexane to give 0.18 g (45%) of $\mathbf{1_{but}}$. Mp 162-164°C. ^{1}H NMR (500 MHz, $CDCl_3$): 8.78 (br. s, 3H), 8.07 (d, *J* 12 Hz, 3H), 7.27-7.34 (m, 6H), 7.08 (t, *J* 7.3 Hz), 6.91 (d, *J* 7.5 Hz, 3H), 3.96 (br. s, 6H), 1.86 (quintet, *J* 6.8 Hz, 6H), 1.79 (s, 18H), 1.53 (sextet, *J* 7.2 Hz, 6H), 1.05 (t, *J* 7.2 Hz, 9H); ^{13}C NMR (125 MHz, $CDCl_3$): 147.4, 143.3, 141.2, 127.9, 122.6, 121.9, 108.7, 99.4, 48.1, 43.4, 29.2, 28.8, 26.9, 20.4, 13.9; HRMS (ESI) m/z calcd for $C_{54}H_{64}N_3O_3$: 802.4948 [MH^+]; found: 802.4940. The results of 2D NOESY experiments and X-Ray crystallographic data confirm that the enamine double bonds in $\mathbf{1_{but}}$ and $\mathbf{1_{met}}$ are all "E" (see Supplementary Information, SI).

2,4,6-tris(2-(1-methylquinolin-2(1H)-ylidene)ethylidene)cyclohexane-1,3,5-trione, 2_{met}: The mixture of 1,2-dimethylquinolin-1-ium iodide[11] (0.47 g, 1.65 mmol), 2,4,6-trioxocyclohexane-1,3,5-tricarbaldehyde (0.11 g, 0.5 mmol), and piperidine (0.25 g, 3 mmol) in 4 ml of pyridine was refluxed for 5 min. After cooling, the reaction was diluted with 40-50 ml of diethyl ether. The solvents were decanted and the oily material was washed several times with diethyl ether. The crude product was eluted through aluminum oxide (CH_2Cl_2-CH_3OH, 98:2) to give 0.17 g (53%) of $\mathbf{2_{met}}$. Mp 260°C (dec.). ^{1}H NMR (mixture of diastereomers, 500 MHz, DMSO-d_6): 8.44-8.54 (m, 3H), 8.06-8.16 (m, 3H), 7.75-7.86 (m, 3H), 7.60-7.75 (m, 12H), 7.27-7.35 (m, 3H), 3.75-3.82 (m, 9H); ^{13}C NMR (mixture of diastereomers, 125 MHz, DMSO-d_6): 186.1, 184.1, 184.0, 182.8, 154.4, 154.1, 153.8, 143.8, 143.3, 142.7, 140.3, 140.2, 140.1, 133.9, 133.5, 133.2, 131.7, 131.6, 131.5, 128.6, 128.5, 128.4, 123.9, 123.8, 123.7, 123.6, 123.4, 120.8, 119.1, 119.0, 118.9, 118.8, 118.7, 117.1, 115.7, 115.6, 115.4, 102.2, 101.7, 35.6, 35.5, 35.4; HRMS (ESI) m/z calcd for $C_{42}H_{34}N_3O_3$: 628.2595 [MH^+]; found: 628.2609. As indicated above in reporting the NMR chemical shifts, and as seen in the spectra shown in the SI, $\mathbf{2_{met}}$ is formed as a mixture of diastereomers. This subtlety will not influence the photophysical measurements at the core of this report. The x-ray structure for $\mathbf{1_{met}}$ (see SI) indicates that the double bonds at the central six-membered ring in this compound are all E. We are uncertain if this is also true for all the other compounds examined. However, as with the mixture of the diastereomers for $\mathbf{2_{met}}$, this uncertainty should not influence the photophysical measurements.

Instrumentation and approach. Published articles describe the laser systems, spectrometers and approaches used to (1) quantify $O_2(a^1\Delta_g)$ yields,[12, 13] (2) monitor triplet state absorption,[14] and (3) perform laser induced optoacoustic calorimetric measurements.[12, 15]

Fluorescence spectra and fluorescence quantum yields, ϕ_f, were determined using a Horiba Jobin Yvon Fluromax P spectrometer. Spectra were corrected for the instrument response. Experiments were performed using 1 cm cuvettes and the sample absorbance at the excitation wavelength was always less than 0.1. All fluorescence quantum yields were determined using *meso*-tetraphenylporphyrin, TPP, in toluene as the standard ($\phi_f = 0.11$)[16] because TPP has appreciable absorption at the same wavelength as compounds **1** and **2**. For these measurements, the entire fluorescence spectrum was integrated and the resultant integral was plotted against the sample absorbance for at least 5 independent samples prepared over the concentration range of 0.2 – 2.0 μM (*i.e.*, absorbance range of 0.01 to 0.1). The quantum yields thus obtained were then confirmed in repeated experiments using different excitation wavelengths.

Cyclic voltammograms were recorded using argon-saturated N,N,dimethylformamide solutions and a three-electrode potentiostat (CH Instruments model CHI-600) equipped with a carbon-glass working electrode, a platinum counter electrode, and a Ag/AgI reference electrode. The concentration of the merocyanine dyes was 1.3×10^{-4} M with 0.1 M tetrabutylammonium tetrafluoroborate as the supporting electrolyte. Half-wave potentials were extracted as the midpoint between the peaks and averaged over different scan rates. The data were converted to the SCE scale using the ferrocene/ferricinium system as a standard.

Absorption spectra were recorded on a Shimadzu UV3600 spectrophotometer.

Results and discussion

All optical and calorimetric experiments were performed using toluene solutions of the merocyanine dyes. Although compounds $\mathbf{2}_{\mathbf{met}}$ and $\mathbf{2}_{\mathbf{but}}$ are less soluble in toluene than compounds $\mathbf{1}_{\mathbf{met}}$ and $\mathbf{1}_{\mathbf{but}}$,[8] amounts sufficient for our experiments could nevertheless be dissolved.

1. Absorption spectra, fluorescence spectra and fluorescence quantum yields

Absorption and fluorescence spectra of the four merocyanine compounds are shown in Fig. 2 and pertinent data are presented in Table 1. The spectra of compound **2** are clearly distinguished from those of compound **1** by an appreciable red shift, as expected for the increased conjugation length in **2**. We likewise observe a significant difference in ϕ_f between compounds **1** and **2**; the efficiency of fluorescence from compound **2** is appreciably less than that in compound **1**. We return to this point in subsequent sections. Although the absolute value of ϕ_f that we obtain for $\mathbf{1}_{\mathbf{met}}$ (0.27 ± 0.03) is appreciably larger than what has previously been reported (0.034),[8] we stand by the accuracy of our present number (see discussion in Experimental Section). However, this difference should not detract from the relative ϕ_f values for compounds **1** and **2** shown in Table 1.

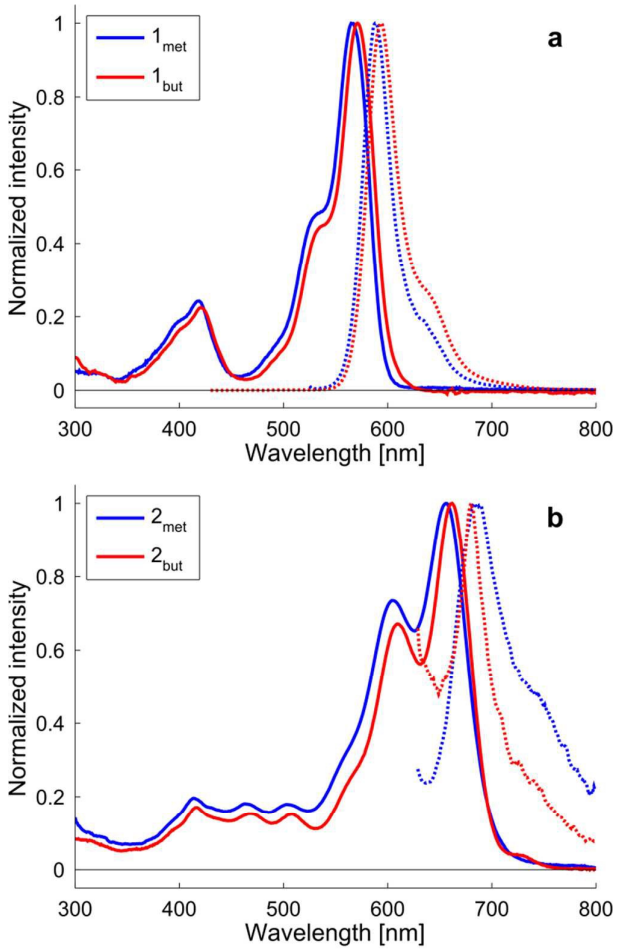

Fig. 2. Absorption (solid lines) and fluorescence (dotted lines) of the merocyanine dyes in toluene. (a) Compounds $\mathbf{1}_{met}$ and $\mathbf{1}_{but}$. (b) Compounds $\mathbf{2}_{met}$ and $\mathbf{2}_{but}$. The apparent increase in emission intensity at shorter wavelengths in panel b is due to scattered light from the excitation source that is readily detected in these weakly fluorescent samples.

Table 1. Photophysical and spectroscopic parameters for compounds **1** and **2** in toluene

Compound	λ_{max} (abs) nm	λ_{max} (ems) nm	α^{oxygen}	$\alpha^{nitrogen}$	ϕ_f	ϕ_Δ
$\mathbf{1}_{met}$	566	588	0.14 ± 0.06	0.15 ± 0.05	0.27 ± 0.03	0.33 ± 0.03
$\mathbf{1}_{but}$	571	594	0.13 ± 0.05	0.10 ± 0.04	0.25 ± 0.02	0.38 ± 0.03
$\mathbf{2}_{met}$	656	684	0.82 ± 0.08	0.84 ± 0.06	0.0005 ± 0.0001	0.0046 ± 0.0005
$\mathbf{2}_{but}$	662	680	0.86 ± 0.07	0.89 ± 0.07	0.0004 ± 0.0001	0.0047 ± 0.0004

2. Quantum yield of $O_2(a^1\Delta_g)$ production

Quantum yields of $O_2(a^1\Delta_g)$ production sensitized by our four merocyanine derivatives were determined using a procedure[17, 18] in which the respective integrated intensities of the time-resolved $O_2(a^1\Delta_g) \rightarrow O_2(X^3\Sigma_g^-)$ phosphorescence signals at 1275 nm were compared to the integrated intensity of the $O_2(a^1\Delta_g) \rightarrow O_2(X^3\Sigma_g^-)$ phosphorescence signal obtained from a reference sensitizer for which ϕ_Δ is known. The standard used was PN ($\phi_\Delta = 0.98 \pm 0.05$),[15, 19] and experiments were performed upon irradiation at 420 nm. Representative data are shown in Fig. 3 and the ϕ_Δ values thus obtained are shown in Table 1. Independent experiments performed with irradiation at 595 nm using TPP as the standard ($\phi_\Delta = 0.66 \pm 0.08$)[6] gave comparable results. The $O_2(a^1\Delta_g)$ lifetimes obtained in these experiments (~ 30 μs) are consistent with what is expected for solvent-mediated deactivation in toluene and indicate that, under our conditions, **1** and **2** do not interact with and quench $O_2(a^1\Delta_g)$.

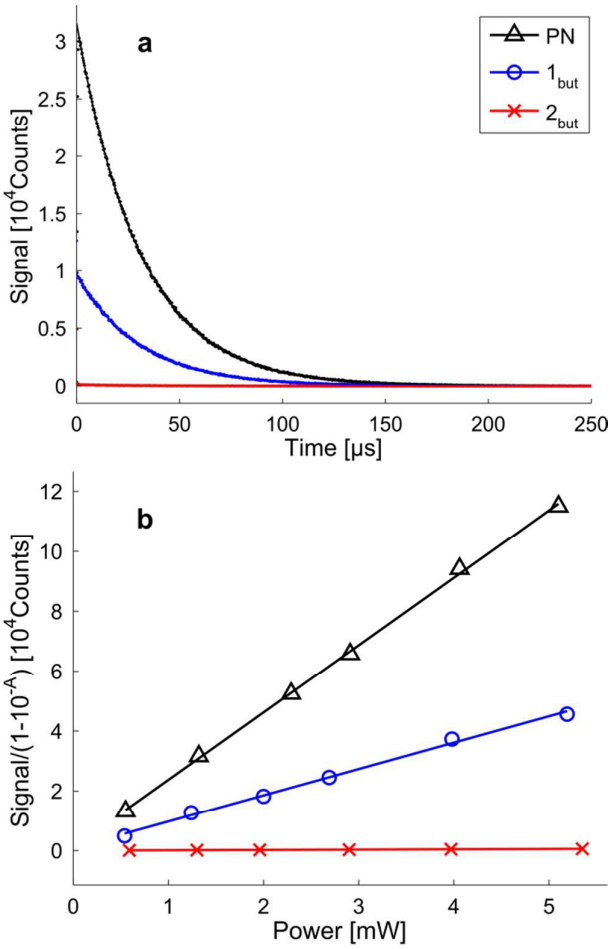

Fig. 3. (a) Representative time-resolved 1275 nm $O_2(a^1\Delta_g)$ phosphorescence traces recorded upon irradiation of the standard sensitizer PN (black line), **1**$_{but}$ (blue line), and **2**$_{but}$ (red line). Although difficult to see, the results of a single exponential fitting function are superimposed on the raw data shown for each kinetic trace. (b) Plots of the absorbance-normalized intensity of the $O_2(a^1\Delta_g)$ phosphorescence signal as a function of the laser power absorbed by these three molecules. The solid lines are linear fits to the data, and the error on a given data point is smaller than the symbol used to indicate that point.

The ϕ_Δ values obtained complement the ϕ_f values for these same compounds; compound **1** photosensitizes the production of $O_2(a^1\Delta_g)$ in much higher yields than compound **2**.

3. Triplet absorption experiments

Time-resolved absorption experiments were performed on solutions of **1** and **2**.

Upon pulsed laser irradiation into the absorption band of **1** in a nitrogen-saturated solution, a transient absorption signal was observed that had a lifetime of ~ 1 ms. The intensity of this signal was greatest at ~ 650 nm. Upon exposing this solution to oxygen, this transient absorption signal disappeared. These observations are consistent with what is expected when monitoring a triplet state. The observation of this oxygen-concentration-dependent absorption signal is consistent with the fact that **1** sensitizes the production of $O_2(a^1\Delta_g)$ in appreciable yield (*i.e.*, $\phi_\Delta \sim 0.3 - 0.4$; Table 1). Thus, we infer that intersystem crossing from the excited singlet to triplet state in **1** occurs with a quantum efficiency of at least ~ 0.3.

Upon pulsed laser irradiation of **2**, corresponding transient absorption signals were not observed. We thus infer that **2** does not intersystem cross from the excited singlet to triplet state with appreciable yield. If we likewise assume that the triplet state of these merocyanines is the precursor to $O_2(a^1\Delta_g)$, then these time-resolved absorption data are consistent with the observation that compound **2** does not photosensitize the production of $O_2(a^1\Delta_g)$ in great yield (Table 1).

4. Laser-Induced Optoacoustic Calorimetry (LIOAC)

The fluorescence, $O_2(a^1\Delta_g)$, and triplet absorption data presented above lead us to infer that compound **2** is more prone to rapid non-radiative deactivation than compound **1**. Indeed, this speculation at the early stages of this project led us to examine the effects of *N*-butylation as opposed to *N*-methylation in these compounds. The intent here was to ascertain whether the addition of extra vibrational and rotational degrees of freedom to this part of the chromophore would influence the fluorescence and $O_2(a^1\Delta_g)$ quantum yields (*i.e.*, the "loose-bolt" effect).[20] As seen in Table 1, this substituent change does not result in an appreciable difference in the $O_2(a^1\Delta_g)$

and fluorescence yields in both **1** and **2**. Thus, other factors must contribute to the apparent difference with which **1** and **2** dissipate electronic excitation energy via non-radiative channels. To put our supposition that **2** is more prone to non-radiative deactivation than **1** on a more quantitative footing, we set out to perform a series of LIOAC experiments.

In the LIOAC experiment, a piezoelectric transducer attached to the sample cuvette is used to record the pressure wave that results as a consequence of the pulsed-laser-induced, time-resolved solvent expansion associated with energy dissipation upon non-radiative deactivation of an excited electronic state.[21] Our experiments were performed (a) with a transducer that had a response time of ~1 μs and (b) using a laser beam of diameter ~1 mm. The latter yields an acoustic transit time of ~ 1 μs in our chosen solvent of toluene (*i.e.*, acoustic transit time = (beam diameter)/(speed of sound)).[21] Under these conditions, any heat released by the solute at time scales faster than ~1 μs is simply convolved into the pressure wave initially observed. Thus, for LIOAC experiments on compounds **1** and **2** performed under oxygen-saturated conditions, where the triplet states of these compounds are fully quenched by oxygen, all heat released directly from **1** and **2** will be reflected in the amplitude of the initial pressure wave. Because the lifetime of $O_2(a^1\Delta_g)$ in toluene is ~ 30 μs, heat release from $O_2(a^1\Delta_g)$ formed as a consequence of these quenching reactions will not appreciably influence the amplitude of this initial pressure wave (*i.e.*, $O_2(a^1\Delta_g)$ is simply an energy storing species on this time scale).

As shown in eqn 1, the amplitude of the initial pressure wave, H, is expressed as a function of the sample absorbance at the irradiation wavelength, A, the incident laser power, P, an instrument- and solvent-dependent proportionality constant, κ, and the fraction of excited state energy released as "fast heat" to the system, α.[21]

$$H = \kappa\alpha P(1 - 10^{-A}) \qquad (1)$$

The parameter α can be quantified for a given molecule using, as a standard, the corresponding pressure wave recorded under identical conditions (*i.e.*, identical κ) from a molecule for which α is known. For our experiments, we chose azulene as our standard; it has an α value of 0.99 ± 0.02 and an appreciable absorbance in the same spectral region as **1** and **2**.[22] Representative LIOAC data obtained in our experiments are shown in Fig. 4.

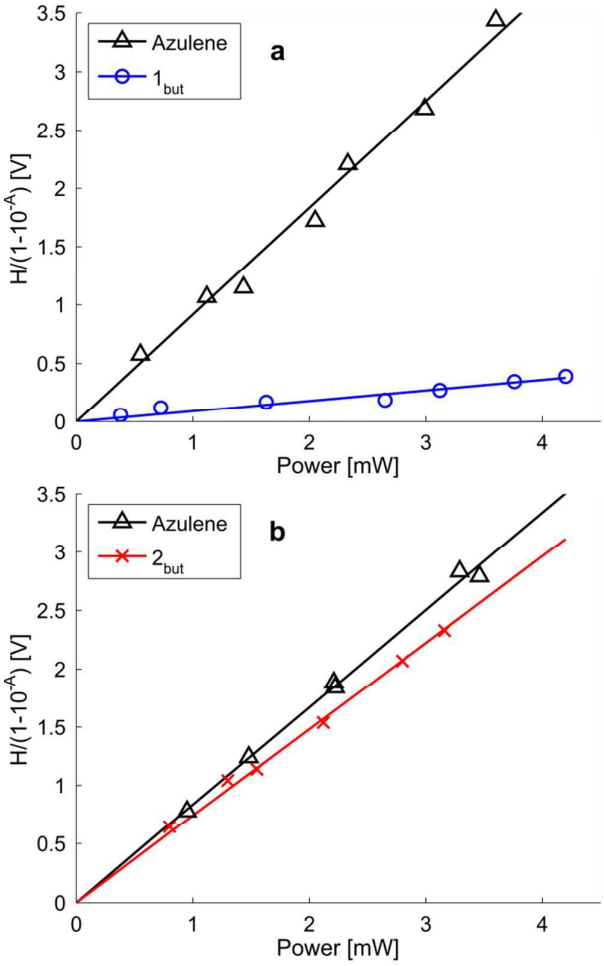

Fig. 4. Plots of the absorbance-corrected peak-to-peak amplitude of the initial LIOAC pressure wave against the incident laser power for nitrogen-saturated solutions of $\mathbf{1}_{\mathbf{but}}$ and $\mathbf{2}_{\mathbf{but}}$ along with the corresponding plot for the standard azulene. Linear fits to the data are shown.

The α values obtained from the data shown in Fig. 4, and the corresponding data from $\mathbf{1}_{\mathbf{met}}$ and $\mathbf{2}_{\mathbf{met}}$, clearly indicate that more of the excitation energy is released as "fast heat" in compounds $\mathbf{2}_{\mathbf{met}}$ and $\mathbf{2}_{\mathbf{but}}$ than in compounds $\mathbf{1}_{\mathbf{met}}$ and $\mathbf{1}_{\mathbf{but}}$ (Table 1). This observation is entirely consistent with the fluorescence and $O_2(a^1\Delta_g)$ quantum yield data also shown in Table 1.

The α values recorded as a function of oxygen concentration also indicate an important point that we address qualitatively here, but more quantitatively in Section 6 below. The observation that α values for $\mathbf{2}_{\mathbf{met}}$ and $\mathbf{2}_{\mathbf{but}}$ are the same in both oxygen- and nitrogen-saturated solutions is consistent with our transient absorption experiments and our $O_2(a^1\Delta_g)$ yields. Specifically, it appears that a long-lived, oxygen-quenchable triplet state is not formed in high yield in $\mathbf{2}_{\mathbf{met}}$ and $\mathbf{2}_{\mathbf{but}}$, and fast heat release derives principally from nonradiative deactivation of the excited singlet state. On the other hand, the observation that α values for $\mathbf{1}_{\mathbf{met}}$ and $\mathbf{1}_{\mathbf{but}}$ are the same in both oxygen- and nitrogen-saturated solutions requires a different explanation simply because an oxygen-quenchable triplet state is formed. In this case, under nitrogen-saturated conditions, fast heat release only comes from the nonradiative deactivation of the singlet state (*i.e.*, internal conversion and intersystem crossing). The resultant triplet state is sufficiently long-lived that it is an energy-storing species on our time scale. Under oxygen-saturated conditions, where all of the $\mathbf{1}_{\mathbf{met}}$ and $\mathbf{1}_{\mathbf{but}}$ triplet states are quenched by oxygen, the observation of an identical α values implies that energy transfer from the triplet states of $\mathbf{1}_{\mathbf{met}}$ and $\mathbf{1}_{\mathbf{but}}$ to form $O_2(a^1\Delta_g)$ occurs with unit efficiency (*i.e.*, recall that $O_2(a^1\Delta_g)$ is likewise a long-lived energy storing species).

5. Photo-induced reactions

To further characterize our systems with respect to the distribution of energy delivered upon light absorption, it is important to ascertain whether these compounds undergo photoinitiated chemical reactions in which bonds are made and/or broken. To this end, we examined the

absorption spectra of both air- and nitrogen-saturated solutions of **1** and, independently, **2** upon prolonged irradiation with the same pulsed laser used in our LIOAC experiments. Representative data shown in Fig. 5 clearly indicate that both **1** and **2** undergo photo-initiated chemical reactions.

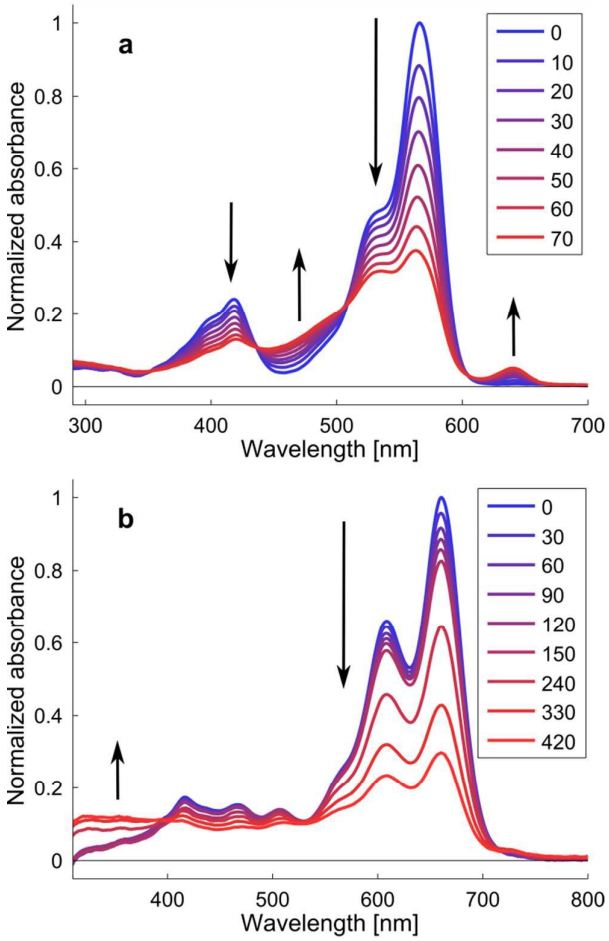

Fig. 5. Absorption spectra of nitrogen-saturated solutions of (a) $\mathbf{1}_{met}$ and (b) $\mathbf{2}_{but}$ recorded as a function of the elapsed exposure time to 100 mW pulsed laser irradiation at 565 nm and 650 nm, respectively. The arrows indicate the direction of photo-induced changes in absorbance and the inset shows the elapsed irradiation time in minutes. Corresponding spectra recorded for $\mathbf{1}_{but}$ showed the same behavior as seen with $\mathbf{1}_{met}$, and the $\mathbf{2}_{met}$ data likewise resembled that recorded from $\mathbf{2}_{but}$. Experiments performed using aerated solutions yielded data very similar to those recorded from nitrogen-saturated solutions.

Data recorded from $\mathbf{1}_{\mathbf{met}}$ and $\mathbf{1}_{\mathbf{but}}$ show distinct isosbestic points suggesting that the photoreaction forms only one product. Although there is precedence for related merocyanines to undergo a photo-induced interconversion with a spiropyran form of the molecule,[23-25] we were not able to regenerate the original spectra assigned to $\mathbf{1}_{\mathbf{met}}$ and $\mathbf{1}_{\mathbf{but}}$ either by changing the sample temperature or by irradiating into the new band at 470 nm. Thus, it is more likely that the data shown in Fig. 5a reflect the irreversible oxygen-independent degradation of $\mathbf{1}_{\mathbf{met}}$ to form a discrete product. In contrast, upon prolonged irradiation of $\mathbf{2}_{\mathbf{met}}$ and $\mathbf{2}_{\mathbf{but}}$, analogous isosbestic points were not observed in the spectra recorded (Fig. 5b). Instead, the bands with characteristic vibronic structure decreased in intensity, to be replaced only by what appears to be a broad band whose maximum is < 400 nm. These data suggest that $\mathbf{2}_{\mathbf{met}}$ and $\mathbf{2}_{\mathbf{but}}$ undergo irreversible fragmentation reactions that disrupt the extensively-conjugated parent compound.

Our data indicate that a non-negligible amount of the incident photon energy is used to make/break bonds in **1** and **2**, and this is useful information in establishing the total "energy budget" for our systems (*vide infra*). It is important to recognize, however, that the LIOAC, ϕ_{Δ}, and ϕ_{f} experiments were all performed under conditions where the photodegradation reactions of **1** and **2** were not noticeable. Specifically, the irradiation powers and exposure times used for these photophysical measurements were far less than what was used to obtain the data in Fig. 5 (*i.e.*, < 5 mW as opposed to 100 mW, < 7 min total exposure time as opposed to > 10 min exposure time). Moreover, we always confirmed that the absorption spectrum of the sample did not change during, and as a consequence of, the photophysical measurement.

6. The energy budget

Given the data in Table 1 and the knowledge that irreversible photochemistry indeed occurs with these compounds, we can now complete our quantitative assessment of how the incident

photon energy is distributed in the respective kinetically-competing excited-state deactivation channels.

For the two experimental conditions of nitrogen-saturated and oxygenated samples, the pertinent expressions based on the conservation of energy are shown as eqns 2 and 3, respectively.

$$E_L\left(1-\alpha^{Nitrogen}\right)=\varphi_F E_F+\varphi_T E_T \exp\left(-\frac{\tau_A}{\tau_T^{Nitrogen}}\right)+E_{Chem}^{Nitrogen} \quad (2)$$

$$E_L(1-\alpha^{Oxygen})=\varphi_F E_F+\varphi_\Delta E_\Delta \exp\left(-\frac{\tau_A}{\tau_\Delta}\right)+E_{Chem}^{Oxygen} \quad (3)$$

Here, E_L is the molar energy of the incident laser light and E_F and E_T are the molar energies of the molecule's excited singlet and triplet states. The 94 kJ/mol excitation energy of $O_2(a^1\Delta_g)$ is E_Δ and the energies associated with the bond making/breaking processes are represented as E_{Chem}. E_F is directly obtained from the crossing point of the scaled absorption and fluorescence spectra shown in Fig. 2. Because E_T and the quantum yield of triplet state production, ϕ_T, are not known, it is prudent to limit our analysis to data recorded from solutions under conditions in which all of the triplet states are rapidly quenched by oxygen (*i.e.*, eqn 3). In this case, as we have indicated, because $\tau_A << \tau_\Delta$, the exponential scaling factor is unity, and we can directly solve for the unknown term E_{Chem}. The resultant data are shown in Table 2.

Table 2. The distribution of the incident photon energy for compounds **1** and **2** expressed as a percentage of the total for data recorded from oxygen-containing solutions

Compound	fast heat release	fluorescence	singlet oxygen production	irreversible chemistry[a]
$\mathbf{1}_{met}$	14 ± 6	27 ± 3	33 ± 3	26 ± 7
$\mathbf{1}_{but}$	13 ± 5	25 ± 2	38 ± 3	24 ± 6
$\mathbf{2}_{met}$	82 ± 8	0. 05 ± 0. 01	0. 46 ± 0. 05	17 ± 8
$\mathbf{2}_{but}$	86 ± 7	0. 04 ± 0. 01	0. 47 ± 0. 04	13 ± 7

a) The errors shown here propagate from the errors in the experimentally determined parameters shown in the other three columns of this table.

7. Electrochemical characterization

The data presented thus far clearly indicate that rapid nonradiative deactivation plays a greater role with the excited singlet states of $\mathbf{2}_{met}$ and $\mathbf{2}_{but}$ than with the excited singlet states of $\mathbf{1}_{met}$ and $\mathbf{1}_{but}$. It remains to provide a reasonable explanation for this observation.

It is established that charge-transfer-mediated coupling between electronic states can facilitate nonradiative deactivation.[26, 27] For a unimolecular process, the pertinent charge transfer (CT) state involves the intramolecular redistribution of electron density (*e.g.*, from the amine to carbonyl moieties in **1** and **2**). For a bimolecular process in which $O_2(X^3\Sigma_g^-)$ collides with an excited state of an organic molecule M, the transfer of electron density from M* to $O_2(X^3\Sigma_g^-)$ can likewise be treated as an intramolecular redistribution within the ephemeral M-O_2 complex.[27] If we assume that the relative ease of forming such CT states correlates with the oxidation/reduction potentials of the organic molecule, then it is desirable to examine the electrochemical behavior of both **1** and **2**.

The data shown in Fig. 6 clearly indicate that compound **2** is more readily oxidized and reduced than compound **1**. This observation is consistent with the fact that the extent of π

conjugation, and hence electron delocalization, is greater in $\mathbf{2}_{met}$ and $\mathbf{2}_{but}$ than in $\mathbf{1}_{met}$ and $\mathbf{1}_{but}$. Thus, a reasonable explanation for the data shown in Table 1 is that CT-mediated nonradiative deactivation of the excited singlet states of $\mathbf{2}_{met}$ and $\mathbf{2}_{but}$ effectively competes against fluorescence, intersystem crossing, and ultimately $O_2(a^1\Delta_g)$ production. In contrast, CT-mediated nonradiative deactivation in $\mathbf{1}_{met}$ and $\mathbf{1}_{but}$ does not as effectively kinetically compete resulting in higher yields of both fluorescence and $O_2(a^1\Delta_g)$. The inference in the latter case is that, with a less easily oxidized/reduced system, the pertinent CT state is higher in energy, and thus less able to mediate coupling between the singlet excited state and the ground state.[27]

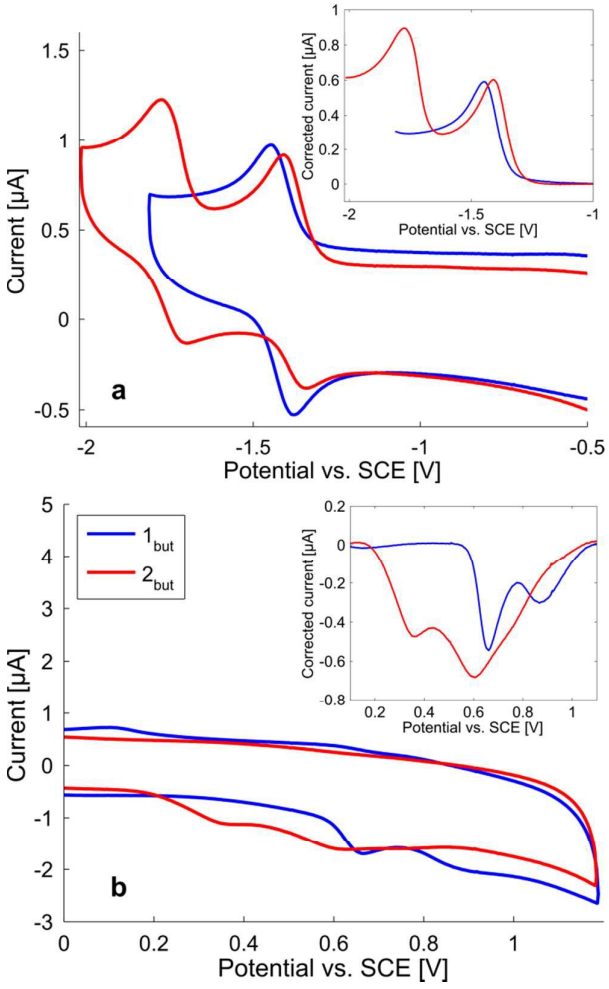

Fig. 6. Reduction (a) and oxidation (b) cyclic voltammograms for compounds $\mathbf{1}_{but}$ (blue line) and $\mathbf{2}_{but}$ (red line) recorded in dimethylformamide. The inserts show background-normalized

sections of the voltammograms to better highlight the potentials at which reduction and oxidation, respectively, occur. The insets also show that the respective peak heights are approximately the same, thus demonstrating that we are oxidizing and reducing the same compound, not an impurity in the sample. Data recorded using $\mathbf{1}_{\mathbf{met}}$ corresponded to that recorded for $\mathbf{1}_{\mathbf{but}}$ and data recorded using $\mathbf{2}_{\mathbf{met}}$ corresponded to the $\mathbf{2}_{\mathbf{but}}$ data.

Conclusion

We have ascertained that a seemingly subtle structural change in the chromophore of an octupolar merocyanine dye can have appreciable effects on the photosensitized yield of $O_2(a^1\Delta_g)$. For the specific molecules examined, replacement of an indoline-based group with a quinoline-based group results in an appreciable increase in the efficiency of nonradiative excited state deactivation. This nonradiative deactivation channel kinetically competes with excited state deactivation channels that result in $O_2(a^1\Delta_g)$ formation. The correlation of such seemingly subtle structure-dependent properties to the yields of photosensitized $O_2(a^1\Delta_g)$ production is a key component that will ultimately help facilitate the rational design of $O_2(a^1\Delta_g)$ photosensitizers with specific properties.

Acknowledgements

This work was supported by the Danish National Research Foundation, the EU Marie Curie Training Program (TopBio PITN-GA-2010-264362), and the Foundation for Polish Science (TEAM-2009-4/3).

References

1 H. K. Ledford and K. K. Niyogi, Singlet oxygen and photo-oxidative stress management in plants and algae, *Plant Cell Environ.*, 2005, **28**, 1037-1045.

2 A. Krieger-Liszkay, Singlet oxygen production in photosynthesis, *J. Expt. Bot.*, 2004, **56**, 337-346.

3 R. Bonnett, *Chemical Aspects of Photodynamic Therapy*, Gordon and Breach Science Publishers, Amsterdam, 2000.

4 C. Schweitzer and R. Schmidt, Physical Mechanisms of Generation and Deactivation of Singlet Oxygen, *Chem. Rev.*, 2003, **103**, 1685-1757.

5 M. Westberg, L. Holmegaard, F. M. Pimenta, M. Etzerodt and P. R. Ogilby, Rational Design of an Efficient, Genetically Encodable, Protein-Encased Singlet Oxygen Photosensitizer, *J. Am. Chem. Soc.*, 2015, **137**, 1632-1642.

6 F. Wilkinson, W. P. Helman and A. B. Ross, Quantum Yields for the Photosensitized Formation of the Lowest Electronically Excited Singlet State of Molecular Oxygen in Solution, *J. Phys. Chem. Ref. Data*, 1993, **22**, 113-262.

7 R. W. Redmond and J. N. Gamlin, A compilation of singlet oxygen yields from biologically relevant molecules, *Photochem. Photobiol.*, 1999, **70**, 391-475.

8 Y. M. Poronik, V. Hugues, M. Blanchard-Desce and D. T. Gryko, Octupolar Merocyanine Dyes: A New Class of Nonlinear Optical Chromophores, *Chem. Eur. J.*, 2012, **18**, 9258-9266.

9 E. Pottier, M. Sergent, R. P. T. Luu and R. Guglielmetti, Synthese De Quelques Spiro[Indoline-Naphtoxazines] Et Spiro [Indoline-Pyridobenzoxazines] Photochromiques., *Bull. Soc. Chim. Belg.*, 1992, **101**, 719-739.

10 J. H. Chong, M. Sauer, B. O. Patrick and M. J. MacLachlan, Highly Stable Keto-Enamine Salicylideneanilines., *Org. Lett.*, 2003, **5**, 3823-3826.

11 M. Wang, M. Gao, K. D. Miller, G. W. Sledge, G. D. Hutchins and Q.-H. Zheng, Simple synthesis of carbon-11 labeled styryl dyes as new potential PET RNA-specific living cell imaging probes, *Eur. J. Medchem.*, 2009, **44**, 2300-2306.

12 J. Arnbjerg, M. Johnsen, P. K. Frederiksen, S. E. Braslavsky and P. R. Ogilby, Two-Photon Photosensitized Production of Singlet Oxygen: Optical and Optoacoustic Characterization of Absolute Two-Photon Absorption Cross Sections for Standard Sensitizers in Different Solvents., *J. Phys. Chem. A*, 2006, **110**, 7375-7385.

13 P. Salice, J. Arnbjerg, B. W. Pedersen, R. Toftegaard, L. Beverina, G. A. Pagani and P. R. Ogilby, Photophysics of Squaraine Dyes: Role of Charge-Transfer in Singlet Oxygen Production and Removal., *J. Phys. Chem. A*, 2010, **114**, 2518-2525.

14 T. Keszthelyi, D. Weldon, T. N. Andersen, T. D. Poulsen, K. V. Mikkelsen and P. R. Ogilby, Radiative Transitions of Singlet Oxygen: New Tools, New Techniques, and New Interpretations., *Photochem. Photobiol.*, 1999, **70**, 531-539.

15 J. Arnbjerg, M. J. Paterson, C. B. Nielsen, M. Jørgensen, O. Christiansen and P. R. Ogilby, One- and Two-Photon Photosensitized Singlet Oxygen Production: Characterization of Aromatic Ketones as Sensitizer Standards., *J. Phys. Chem. A*, 2007, **111**, 5756-5767.

16 P. Seybold and M. Gouterman, Porphyrins XIII: Fluorescence Spectra and Quantum Yields, *J. Mol. Spectros.*, 1969, **31**, 1-13.

17 R. D. Scurlock, S. Nonell, S. E. Braslavsky and P. R. Ogilby, Effect of Solvent on the Radiative Decay of Singlet Molecular Oxygen ($a^1\Delta_g$), *J. Phys. Chem.*, 1995, **99**, 3521-3526.

18 R. D. Scurlock, D. O. Mártire, P. R. Ogilby, V. L. Taylor and R. L. Clough, Quantum Yield of Photosensitized Singlet Oxygen ($a^1\Delta g$) Production in Solid Polystyrene, *Macromolecules*, 1994, **27**, 4787-4794.

19 R. Schmidt, C. Tanielian, R. Dunsbach and C. Wolff, Phenalenone, a Universal Reference Compound for the Determination of Quantum Yields of Singlet Oxygen Sensitization, *J. Photochem. Photobiol., A: Chem.*, 1994, **79**, 11-17.

20 N. J. Turro, V. Ramamurthy and J. C. Scaiano, *Principles of Molecular Photochemistry*, University Science Books, Sausalito, 2009.

21 S. E. Braslavsky and G. E. Heibel, Time-Resolved Photothermal and Photoacoustic Methods Applied to Photoinduced Processes in Solution, *Chem. Rev.*, 1992, **92**, 1381-1410.

22 T. Suzuki, Y. Kajii, K. Shibuya and K. Obi, Calorimetric standards for photothermal methods in ultraviolet and visible spectral regions., *Res. Chem. Intermed.*, 1991, **15**, 261-270.

23 N. P. Ernsting, Transient Optical Absorption Spectroscopy of the Photochemical Spiropyran-Merocyanine Conversion, *Chem. Phys. Lett.*, 1989, **159**, 526-531.

24 A. K. Chibisov and H. Görner, Photoprocesses in Spiropyran-Derived Merocyanines, *J. Phys. Chem. A.*, 1997, **101**, 4305-4312.

25 J. Buback, M. Kullmann, F. Langhojer, P. Nuernberger, R. Schmidt, F. Würthner and T. Brixner, Ultrafast Bidirectional Photoswitching of a Spiropyran, *J. Am. Chem. Soc.*, 2010, **132**, 16510-16519.

26 S. P. McGlynn, T. Azumi and M. Kinoshita, *Molecular Spectroscopy of the Triplet State*, Prentice-Hall, Englewood Cliffs, 1969.

27 P.-G. Jensen, J. Arnbjerg, L. P. Tolbod, R. Toftegaard and P. R. Ogilby, Influence of an Intermolecular Charge-Transfer State on Excited-State Relaxation Dynamics: Solvent Effect on the Methylnaphthalene-Oxygen System and its Significance for Singlet Oxygen Production., *J. Phys. Chem. A*, 2009, **113**, 9965-9973.

Table of Contents Graphic: